

Collisional decay of a strongly driven Bose-Einstein condensate

N. Katz, E. Rowen, R. Ozeri*, and N. Davidson

*Department of Physics of Complex Systems,
Weizmann Institute of Science, Rehovot 76100, Israel*

(Dated: November 21, 2018)

We study the collisional decay of a strongly driven Bose-Einstein condensate oscillating between two momentum modes. The resulting products of the decay are found to strongly deviate from the usual s-wave halo. Using a stochastically seeded classical field method we simulate the collisional manifold. These results are also explained by a model of colliding Bloch states.

PACS numbers: 03.75.Kk, 03.75.Lm, 32.80.-t

The decay of many-body states coupled to a quasi-continuum of collisional products is a topic of great experimental and theoretical interest [1, 2]. Experimental Bose-Einstein condensation (BEC) allows us to investigate this decay in detail by use of highly controlled optical lattice potentials. Both the coherent evolution of the condensate in the lattice, and the nature of the quasi-continuum can be manipulated and quantified [3].

The finite lifetime of perturbative bulk excitations in BEC, namely Beliaev and Landau damping, has been extensively studied [4, 5, 6, 7] and is rather well understood. These studies were extended recently to the ground state of a BEC in an optical lattice, and weak excitations over such a state, using band theory formulation [8, 9, 10].

Coherent Rabi oscillations of the condensate between two (or more) macroscopically-populated momentum states can be driven by a strong moving optical lattice potential. These oscillations are described as beating between Bloch states belonging to different bands of the lattice [11, 12]. Due to interaction nonlinearity, a superposition of two such beating Bloch states no longer solves the time-dependent Schrödinger equation, and thus the expected spectra and dynamics are richer than for a single Bloch state [13]. The decay of these excited states cannot be described by mean-field theory nor as an interaction between perturbative Bogoliubov quasi-particles [14] as in the Beliaev formalism.

In this letter we study the collisional decay of such a strongly driven BEC undergoing coherent Rabi oscillations between momentum states by a resonant two-photon Bragg process [15]. We measure a clear deviation of the collisional products from the s-wave halo observed for collisions of a weak excitation with the BEC [1]. Using a stochastically seeded classical field Gross-Pitaevskii equation (GPE) simulation [16], we observe similar decay dynamics. These results are then explained by a model which includes collisions between Bloch states of the optical lattice as a perturbation.

As in [17], our nearly pure ($\sim 95\%$) BEC of $N = 1.6(\pm 0.5) \times 10^5$ ^{87}Rb atoms in the $|F, m_f\rangle = |2, 2\rangle$ ground state, is formed in a magnetic trap with radial and axial trapping frequencies of $\omega_r = 2\pi \times 226$ Hz and $\omega_z = 2\pi \times 26.5$ Hz, respectively, leading to a healing length $\xi = 0.23 \mu\text{m}$. The condensate is driven by a pair of strong Bragg beams counter-propagating along the axial direction \hat{z} , with wavenumbers $k_{d1} = -k_L$ and $k_{d2} = k_L$, with $k_L = 2\pi/780$ nm. The laser frequency is red-detuned 44 GHz from the ^{87}Rb D₂ transition in order to avoid spontaneous emission. The depth of the resulting optical lattice potential is characterized by the two-photon Rabi frequency Ω_d . For strong excitations the mean-field shift is largely suppressed [12], due to temporal averaging of the shift to zero during a cycle of oscillation, and hence the frequency difference between the dressing beams (in the laboratory frame) is set to $\delta_d = 2\pi \times 15$ kHz, the free-particle resonance. This leads to Rabi-like oscillations between the momentum states $k = 0$ and $k = 2k_L$.

The oscillation in the momentum of the atoms is apparent in Fig. 1, where we plot the measured average momentum per particle in the \hat{z} direction as a function of time, extracted from time of flight images. The oscillation frequency, as obtained by a decaying sinusoidal fit, is $\Omega_d/2\pi = 8.6$ kHz.

In the strongly driven condensate, both finite size broadening, and inhomogeneous density broadening are greatly suppressed [12]. Therefore the decay of the oscillations is mostly due to the collisions between atoms in momentum modes 0 and $2\hbar k_L$. The products of such a collision have an average momentum of $\hbar k_L$, and do not, in general, oscillate any more in momentum space. For a Bogoliubov excitation, which is a weak excitation of momentum $2\hbar k_L$ over a large condensate of zero momentum, the collisional products are known to be located on a shell in momentum space, known as the s-wave halo. This shell is the surface in momentum space, conserving both energy and momentum for the collision. Due to the Bogoliubov dispersion relation, which is quadratic for $2k_L\xi > 1$, this shell is nearly spherical.

In our experiment, however, the condensate is *strongly* driven at large momentum $2k_L\xi = 3.9$, and collisions

*Current address: Time and Frequency Division NIST 325 Broadway Boulder, Colorado 80305, USA

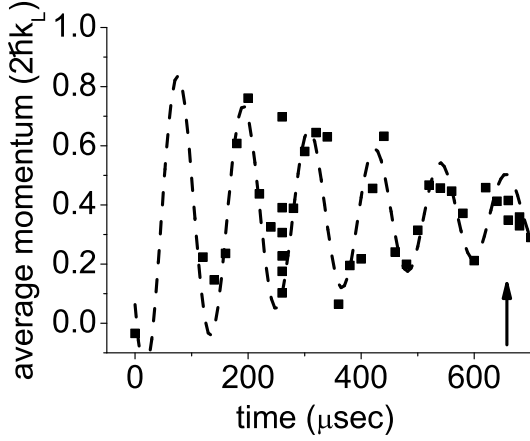


FIG. 1: Average momentum per particle contained in the atomic cloud as a function of time (in units of $2\hbar k_L$, in the laboratory reference frame). Oscillations are due to a strong moving optical lattice which is suddenly switched on, leading to Rabi oscillations between momentum wavepackets. The decay in the oscillations (fit by the dashed line) is mainly due to collisions which deplete the condensate. The arrow marks the point at which Fig. 2(a) (and the subsequent theoretical figures) are taken.

occur within the lattice potential. Consequently, the Bogoliubov description is no longer adequate. This is clearly visible in Fig. 2(a), which shows an absorption image obtained after a resonant dressing pulse lasting $t = 660 \mu\text{s}$. Upon comparison with the s-wave sphere obtained when two condensates collide [Fig. 2(b)], one sees a clear shift of the collided atoms towards the center of the sphere. To quantify this difference we employ computerized tomography to extract the radial dependence of the density from the column-density available in the absorption image [18]. In Fig. 2(c) we plot the radial distribution of atoms over a small slice in \hat{z} . This inward shift of collided atoms is robust and is clearly observed for different values of Ω_d and t .

We qualitatively simulate this collisional decay using the stochastically seeded classical field method, in 2D, as it was developed recently for colliding BECs [16]. In this method the initial seed of fluctuating random amplitudes of the bosonic field is added to the ground state of the condensate in the harmonic trap. Then the moving lattice potential is switched on suddenly (as in the experiment). Matter wave mixing between the condensate momentum wavepackets and the seeded quasi-continuum drives the collisional decay of the oscillations, without any need for further gross numerical intervention. Fig. 3(a) shows the resulting momentum distributions for collisions occurring within the lattice, and Fig. 3(b) shows the collisional manifold when only a weak lattice is present. We note that the overall agreement between the simulation and experiment takes into account

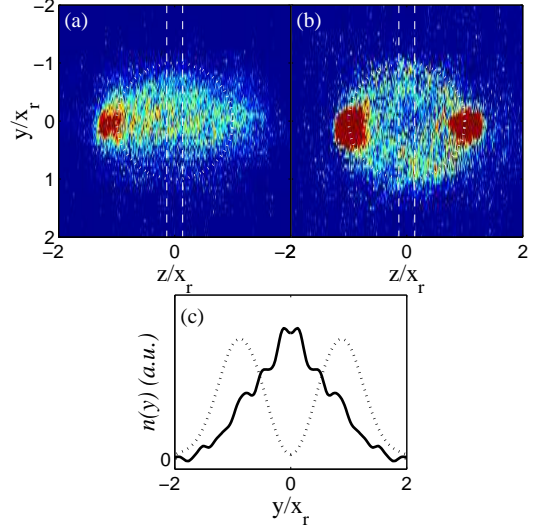


FIG. 2: (a,b) Absorption images after $t_{\text{tof}} = 38 \text{ ms}$ time of flight following a resonant dressing pulse. (a) Strong pulse $\Omega_d/2\pi = 8.6 \text{ kHz}$, pulse width $t = 660 \mu\text{s}$ (b) Weak pulse $\Omega_d/2\pi < 2 \text{ kHz}$, pulse width $t = 370 \mu\text{s}$. Dotted circles represent the predicted s-wave shell. $x_r = \hbar k_L/M \times t_{\text{tof}}$ is the ballistic expansion distance of an atom with wavenumber k_L (in lattice frame of reference). The collisional manifold for the strong pulse is clearly shifted inwards as compared to that of the weak pulse, which agrees with the expected s-wave shell. (c) The density distribution along the y -axis obtained by computerized tomography [18] of the data in (a,b) averaged over a slice marked by the vertical dashed lines. The solid line is for the strongly driven BEC of (a), and the dotted line is for the weakly excited BEC (b). The collisional products of the strongly driven BEC are clearly driven towards the center, while those of the weakly driven BEC are concentrated on the s-wave sphere ($y = x_r$).

many possible systematic effects such as the harmonic confinement in the radial dimension and finite time of the Bragg pulse. We also see that the essential physics is qualitatively captured here, even though the simulation is not in 3D. The correlations between counter-propagating momentum wavepackets, clearly visible in the simulation, are not visible in the experiment due to the fact that the experimental absorption images integrate over an additional dimension, making this signal difficult to observe. The mean-field broadening of the experimental time-of-flight images also leads to some additional smearing.

To obtain an intuitive model that still captures the essence of these phenomena, we neglect inhomogeneous and finite-size effects and choose our frame of reference as moving with the optical lattice of the Bragg lattice beams at velocity $v = -\hbar k_L/M$ along \hat{z} . Our system is then described by the many-body time-independent Hamiltonian

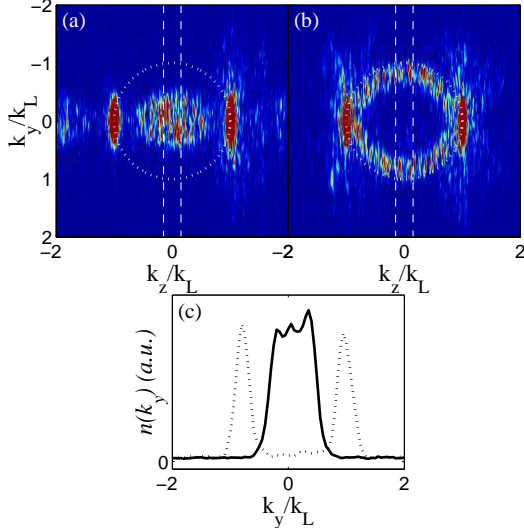


FIG. 3: (a,b) Momentum distributions generated by the classical field GPE simulation (a) Strong pulse $\Omega_d = 8.6$ kHz, pulse width $t = 660 \mu s$ (b) Weak pulse $\Omega_d < 2$ kHz, pulse width $t = 370 \mu s$. The strong lattice leads to a clear shift of the collisional products inward as compared to the weak pulse, and deviates strongly from the s-wave collisional sphere. Note that the simulation also generates momentum wavepackets with clear number correlations. (c) The density distribution along the y -axis, of the simulation, averaged over a slice marked by the vertical dashed lines. The solid line is for the strongly driven BEC of (a), and the dotted line is for the weakly excited BEC (b). The inward shift, observed in the experiment [Fig. 2(c)], of the decay products is even more pronounced here.

$$H = \sum_{\mathbf{k}} \left[\frac{\hbar^2 k^2}{2M} \hat{a}_{\mathbf{k}}^\dagger \hat{a}_{\mathbf{k}} + \frac{\hbar \Omega_d}{2} \left(\hat{a}_{\mathbf{k}}^\dagger \hat{a}_{\mathbf{k}-2\mathbf{k}_L} + \hat{a}_{\mathbf{k}}^\dagger \hat{a}_{\mathbf{k}+2\mathbf{k}_L} \right) \right] + \frac{g}{2V} \sum_{\mathbf{k}, \mathbf{l}, \mathbf{m}} \hat{a}_{\mathbf{k}}^\dagger \hat{a}_{\mathbf{l}}^\dagger \hat{a}_{\mathbf{m}} \hat{a}_{\mathbf{k}+\mathbf{l}-\mathbf{m}}, \quad (1)$$

where $\hat{a}_{\mathbf{k}}^\dagger$ ($\hat{a}_{\mathbf{k}}$) is the creation (annihilation) operator of a particle with wave-vector \mathbf{k} , and g is a constant describing the s-wave interactions. The relative momentum in the experiment is sufficiently low to avoid higher partial wave collisional terms [19, 20]. Neglecting for the moment the interaction term, Eq. (1) simplifies into a one-dimensional single particle Hamiltonian,

$$H = -\frac{\hbar^2}{2M} \frac{\partial^2}{\partial z^2} + \hbar \Omega_d \cos(2k_L z). \quad (2)$$

According to Bloch's theorem, a state $|k\rangle_w$ is only coupled to states $|k + 2pk_L\rangle_w$, where p is an integer. In the moving frame of reference, the stationary BEC has momentum $\hbar k_L$ and is situated on the Brillouin zone boundary. The initial kinetic energy of the condensate is therefore in the lattice energy gap. To calculate the consequent dynamics we span the state $|k_L\rangle_w$ by the new basis

of Bloch states $|n\rangle_b = \sum_p a_n((2p+1)k_L)|((2p+1)k_L)_w$, which diagonalize the Hamiltonian (2) [11], where n is the Bloch band index. The lattice momentum $\hbar q = \hbar k_L$ remains unchanged and is therefore omitted. The subscript w and b indicate whether the quantum numbers in the ket describe the wavenumber of a plane-wave or a Bloch band index.

In the weak lattice limit, we arrive at the two state result $|k_L\rangle_w = 1/\sqrt{2}(|1\rangle_b + |2\rangle_b)$, of a two level system undergoing Rabi oscillations with frequency Ω_d . This two mode picture is still useful even for stronger lattices, since the energy separation between the lower two bands to the third band, on the edge of the Brillouin zone, is typically larger than the Ω_d 's discussed here. Therefore, the higher bands are only weakly occupied by the system.

We now consider the mixing of Bloch states due to atomic interactions. In order to describe collisions, we include the interaction term in the Hamiltonian (1), which scatters two atoms from the populated states. We focus on the processes in which atoms are scattered into the quasi-continuum of unpopulated states, neglecting scattering into populated states (forward scattering) [21]. Since collisions are binary the Hilbert space is reduced to a two particle space. Hamiltonian (1) can be rewritten in the basis of the Bloch Hamiltonian (2) as

$$H = \sum_{\nu_1, \nu_2} |\nu_1; \nu_2\rangle \langle \nu_1; \nu_2| [E_{\nu_1} + E_{\nu_2}] + \frac{g}{2V} \sum_{\mathbf{k}_1 \dots \mathbf{k}_4, \nu_1 \dots \nu_4} \langle \nu_1 | \mathbf{k}_1 \rangle \langle \nu_2 | \mathbf{k}_2 \rangle \langle \mathbf{k}_3 | \nu_3 \rangle \langle \mathbf{k}_4 | \nu_4 \rangle \times |\nu_1, \nu_2\rangle \langle \nu_3, \nu_4 | \delta(\mathbf{k}_1 + \mathbf{k}_2) - (\mathbf{k}_3 + \mathbf{k}_4). \quad (3)$$

Here ν_i stands for all quantum numbers of a Bloch state $n_i, q_i, \mathbf{k}_{i\perp}$. $E_{\nu_i} = E_{n,q} + (\hbar k_{i\perp})^2 / 2M$ is the energy of the noninteracting Bloch state, where $E_{n,q}$ is an eigenvalue of the Bloch Hamiltonian (2) and $\mathbf{k}_{i\perp}$ is the part of \mathbf{k}_i which is perpendicular to \hat{z} [22]. The inclusion of the quantum numbers $\mathbf{k}_{i\perp}$ is necessary since collided atoms gain momentum which is not along \hat{z} . We treat the collision term in Eq. (3) by use of perturbation theory [23]. That is, we assume the system is undergoing coherent oscillations in time due to the lattice potential, and study the perturbative collisional products that are created by the interaction Hamiltonian.

The existence of two macroscopically occupied, distinct energy states, implies several decay routes for the collisional term, and the subsequent energy and momentum conservation manifold are split. Specifically, splitting arises from the energy difference between the case where both colliding atoms are from the $n = 1$ band and when both are from the $n = 2$ band. Due to symmetry, destructive interference suppresses collisions in which there is initially one atom in each of the two bands.

The prediction of our model for the momentum distribution of the collisional products is plotted in Fig. 4.

The calculated column density is presented for comparison with Fig. 2.

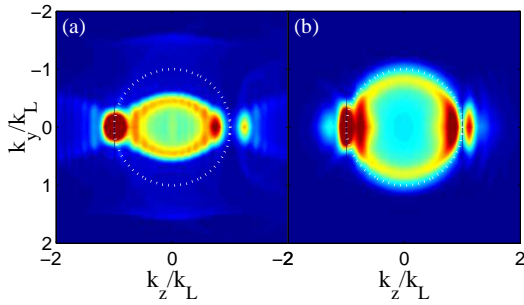


FIG. 4: Column momentum distribution for the same parameters as for Fig. 2(a) and 2(b) respectively calculated by our colliding Bloch state model (Eq. 3, only the scattered atoms are shown). Dotted line represents the s-wave shell. The momentum distribution is only roughly equivalent to the spatial distributions of Fig. 2 due to interactions during expansion, although the overall shape of the collisional manifold is reproduced.

The presence of the optical lattice is found to drive the collided atoms towards the center, as expected from the inner shell of the splitting. The amplitude of the outer shell decreases rapidly as Ω_d increases, and is experimentally unobservable for our parameters. In the experimental data additional effects such as inhomogeneous broadening and mean-field expansion effects, that are neglected in this model, tend to broaden the shell of atoms, and blot out the splitting for smaller Ω_d .

One intriguing prediction of the model, is that the decay rate as a function of time will deviate significantly from that predicted by the Fermi golden rule. This can be explained in the time domain by the oscillatory behavior of the coherent evolution, leading to a complementary oscillation in the rate of production of collided atoms.

Another important result of the model is that as we increase Ω_d , the overall decay of the coherent evolution is accelerated. This is due to the large number of additional decay pathways that are switched on by the presence of a deeper lattice.

In conclusion, we measure the collisional decay of a driven condensate and show that it deviates from the usual s-wave sphere. This result is modelled by using the stochastically seeded classical field method applied to the Gross-Pitaevskii simulation of the experiment. The main features of the collisional decay manifold are captured by a simple model, which treats the interactions as binary collisions between single particle Bloch states.

This work was supported in part by the Israel Ministry of Science, the Israel Science Foundation, and the DIP Foundation. We thank C. Gardiner and A. Norrie for useful discussions.

- [1] W. Ketterle and S. Inouye, *Compte rendus de l'academie des sciences, Serie IV - Physique Astrophysique*, vol. 2, 339 (2001).
- [2] R. Ozeri, N. Katz, J. Steinhauer and N. Davidson, *Rev. Mod. Phys.* **77**, 187 (2005).
- [3] I. E. Mazets, G. Kurizki, N. Katz, N. Davidson, *Phys. Rev. Lett.* in press, cond-mat/0411301 (2005).
- [4] S. T. Beliaev, *Soviet Physics JETP* 34(7) **2**, 299 (1958).
- [5] N. Katz, J. Steinhauer, R. Ozeri and N. Davidson, *Phys. Rev. Lett.* **89**, 220401 (2002).
- [6] E. Hodby, O. M. Marago, G. Hechenblaikner and C. J. Foot, *Phys. Rev. Lett.* **86**, 2196 (2001).
- [7] D. S. Jin, M. R. Matthews, J. R. Ensher, C. E. Wieman and E. A. Cornell, *Phys. Rev. Lett.* **78**, 764 (1997).
- [8] M. Kraemer, C. Menotti, L. Pitaevskii and S. Stringari, *Eur. Phys. J. D* **27**, 247 (2003); D. I. Choi and Q. Niu, *Phys. Rev. Lett.*, **82**, 2022 (1999); B. Wu and Q. Niu, *Phys. Rev. A* **64**, 061603(R) (2001).
- [9] L. Fallani, L. De Sarlo, J. E. Lye, M. Modugno, R. Saers, C. Fort, and M. Inguscio, *Phys. Rev. Lett.* **93**, 140406 (2004).
- [10] O. Morsch, J. H. Müller, M. Cristiani, D. Ciampini and E. Arimondo, *Phys. Rev. Lett.* **87**, 140402 (2001).
- [11] J. Hecker Denschlag et al., *J. Phys. B* **35**, 3095 (2002); A. S. Mellish, G. Duffy, C. McKenzie, R. Geursen, and A. C. Wilson, *Phys. Rev. A* **68**, 051601(R) (2003).
- [12] N. Katz, R. Ozeri, E. Rowen, E. Gershnabel and N. Davidson, *Phys. Rev. A* **70**, 033615 (2004).
- [13] J. Higbie and D. M. Stamper-Kurn, *Phys. Rev. Lett.* **88**, 090401 (2002).
- [14] R. Ozeri, N. Katz, J. Steinhauer, E. Rowen and N. Davidson, *Phys. Rev. Lett.*, **90**, 170401 (2003).
- [15] J. Stenger et al., *Phys. Rev. Lett.* **82**, 4569 (1999).
- [16] A. A. Norrie, R. J. Ballagh, and C. W. Gardiner, *Phys. Rev. Lett.* **94**, 040401 (2005).
- [17] J. Steinhauer, R. Ozeri, N. Katz and N. Davidson, *Phys. Rev. Lett.* **88**, 120407 (2002).
- [18] R. Ozeri, J. Steinhauer, N. Katz and N. Davidson, *Phys. Rev. Lett.* **88**, 220401 (2002).
- [19] N. R. Thomas, N. Kjaergaard, P. S. Julienne, and A. C. Wilson *Phys. Rev. Lett.* **93**, 173201 (2004).
- [20] Ch. Buggle, J. Léonard, W. von Klitzing, and J. T. M. Walraven *Phys. Rev. Lett.* **93**, 173202 (2004).
- [21] Although the weight of such processes is of order N larger than the former, this approach is justified by the observation that the meanfield shift is being averaged out by the rapid oscillations [12]. Its contribution is therefore suppressed.
- [22] In general each interaction term in Eq. (3) should be multiplied by an appropriate bosonic amplification factor. However, in our system there are two approximately equally populated initial Bloch states and target states are assumed to be empty, therefore all terms in Eq. (3) should be multiplied by the same $\sim N/2$.
- [23] Using a 3D simulation of the classical collisional and expansion dynamics, we estimate that less than 10 percent of the atoms in Fig. 2(c) underwent secondary collisions, and therefore the distribution is dominated by single collisions as discussed in our model.